Bioorganic & Medicinal Chemistry Letters 19 (2009) 5009–5011

Contents lists available at ScienceDirect

Bioorganic & Medicinal Chemistry Letters

journal homepage: www.elsevier.com/locate/bmcl

Characterization of α-nitromethyl ketone as a new zinc-binding group based on structural analysis of its complex with carboxypeptidase A

Shou-Feng Wang [a], Guan Rong Tian [a,*], Wen-Zheng Zhang [b], Jing-Yi Jin [a,*]

[a] Key Laboratory of Biological Resources and Functional Molecules of the Changbai Mountains of Ministry of Education, Yanbian University, Yanji, Jilin 133002, China
[b] Institute of Biophysics, Chinese Academy of Science, Beijing 100871, China

ARTICLE INFO

Article history:
Received 10 April 2009
Revised 22 June 2009
Accepted 9 July 2009
Available online 12 July 2009

Keywords:
Zinc-binding group
Crystal structure
Transition-state analog

ABSTRACT

Zinc-binding groups (ZBGs) are exhaustively applied in the development of the new inhibitors against a wide variety of physiologically and pathologically important zinc proteases. Here the α-nitro ketone was presented as a new ZBG, which is a transition-state analog featured by the unique bifurcated hydrogen bonds at the active site of carboxypeptidase A based on the structural analysis. Introduction of a nitro group at the α-position of the ketone could provide more non-covalent interactions without loss of the abilities to form a tetrahedral transition-state analog.

Zinc proteases are a family of enzymes having a catalytically essential zinc ion at their active sites. They include a variety of physiologically and pathologically important species, such as angiotensin-converting enzyme (ACE) and matrix metalloproteases, which are the most studied drug design targets.[1,2] The inhibitor design strategies widely applied to these zinc proteases generally make use of a zinc-binding group (ZBG) that can form coordinative bonds to the zinc ion at the active site of the enzymes, which are usually lessons from the inhibition of carboxypeptidase A (CPA, EC 3.4.17.1) as a leading representative.[3–5] For example, captopril,[6] an inhibitor of ACE, was discovered by application of the design strategy that originated from 2-benzylsuccinic acid as a potent inhibitor of CPA.[7] The other important implication is that the interactions of ketones with CPA were regarded as a model for the inhibition of ACE by carbonyl compounds.[8] Introduction of an α-substituent with strong electron-withdrawing abilities could enhance the electrophilicity of the carbonyl, which facilitated the addition of a nucleophile followed by the formation of a hybridized adduct that mimics the transition state (TS) occurring during normal substrate hydrolysis catalyzed by CPA. For example, α-bromo ketone compound is a TS analog inhibitor of CPA but the non-modified ketone is a substrate analog inhibitor.[9,10] Because the TS analogs utilize the binding energies more effectively, such ZBGs derived inhibitors have been in extensive attentions as potential candidate of drug.[1]

Nitro is a well-known electron-withdrawing group; besides, it could form various hydrogen bonds with the residues at the active site of CPA as shown in the previous report.[11] As expected, introduction of the nitro group at the α-position of the ketone should not only remain the abilities to reach a TS mimic but also provide additional interactions with the residues at the active site of CPA. Therefore, we designed 2-benzyl-5-nitro-4-oxopentanoic acid **5** as the CPA inhibitor. Based on the structural analysis of the CPA-**5** complex, we here present α-nitromethyl ketone as a new TS analog ZBG.

All three optically active forms of **5** (*RS*, *R*, *S*) were synthesized as shown in Scheme 1.[12] Their inhibitory activities against CPA were evaluated and the corresponding inhibitory constant (K_i) values are collected in Table 1.[13] Firstly, it could be found that the K_i values of the series of ketone-based inhibitors against CPA decreased with the increase of the p*K*a values of the same substituted

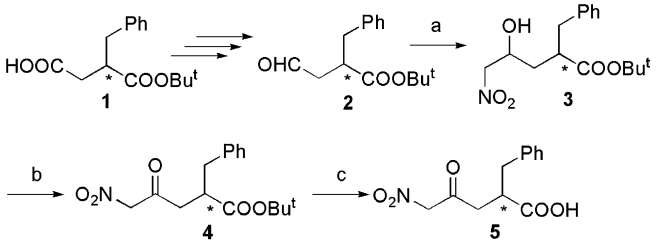

a. CH_3NO_2, KF; b. pyridinium chlorochromate; c. trifluoroacetic acid.

Scheme 1. Synthesis of 2-benzyl-5-nitro-4-oxopentanoic acid.

* Corresponding authors. Tel.: +86 4332732286; fax: +86 4332732456 (J.-Y.J.); tel.: +86 4332762289; fax: +86 4332732456 (G.R.T.).
E-mail addresses: grtn@ybu.edu.cn (G.R. Tian), jyjin-chem@ybu.edu.cn (J.-Y. Jin).

0960-894X/$ - see front matter © 2009 Elsevier Ltd. All rights reserved.
doi:10.1016/j.bmcl.2009.07.060

Table 1

Compound		K_i (μM)	pK_a[14]
		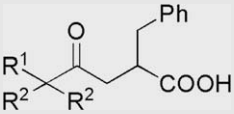	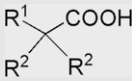
RS-**7**	$R^1 = R^2 = H$	207	4.76
RS-**8**	$R^1 = Br$, $R^2 = H$	15	2.90
RS-**9**[9]	$R^1 = R^2 = F$	0.2	0.50
RS-**5**	$R^1 = NO_2$, $R^2 = H$	0.43	1.68
R-**5**		0.16	
S-**5**		31	

acetic acids (Table 1),[14] which suggest that the electron-withdrawing abilities of the α-substituents should be the key to the inhibitory potency of the ketone-based inhibitors. Kinetic assay of compound **5** as inhibitors against CPA also disclosed that *R*-**5** is the most potent inhibitor with inhibitory constant as 0.16 μM, which is consistent to the L-specificity of CPA.

We are mainly interested in the binding mode of the α-nitromethyl ketone at the active site of CPA. Crystals of the CPA-*R*-**5** complex for X-ray diffraction were then obtained by soaking CPA crystals into the solution containing racemic **5** and determined at a resolution of 1.85 Å (PDB code: 3FX6).[15] The final model including all residues of CPA and *R*-**5** was refined in the range of 50.0–1.85 Å (Table 2). Figure 1 depicts the stereoview of the difference electron density in the region of the active site of CPA that is occupied by *R*-**5**. Distances of important interactions between CPA and *R*-**5** in the complex are listed in Table 3. Structural analysis firstly disclosed that *R*-**5** occupies the S1′ subsite of CPA, where the benzyl moiety resides in the hydrophobic pocket and the carboxylate makes a salt link with the guanidinium group of Arg-145. Tyr-248 is found in the 'so-called' down position, which is responsible to the formation of the hydrophobic pocket. Such binding modes are commonly observed in X-ray crystal structures of CPA-inhibitor complexes.[16] It is also clearly observed that the ketonic hydrate of the *R*-**5** are bound at the active site of CPA. The so-called '*gem*-diol' form with tetrahedron configuration exhibits the structurally essential features of the transition state, that is, a bidentate chelation to the zinc ion and two respective hydrogen bonds with Glu-270 and Arg-127.[17] Thus, the presented *R*-**5** should be a TS analog inhibitor of CPA. Besides the above structural features generally found in the complexes of CPA and its TS analog inhibitors, the introduced nitro group also forms various hydrogen bonding with the residues at the active site of CPA as expected. Both Arg-127 and Arg-71 are involved in the hydrogen bond with the oxygen (O^5) of the nitro group. Thus, the bifurcated hydrogen bond is the other salient structural feature of the CPA-*R*-**5** complex, which should be ascribed to the introduction of the nitro group (Fig. 2).

In conclusion, we successfully introduced the nitro group to the ketone skeleton and then developed α-nitromethyl ketone as a new ZBG. The presented ketone-based ZBG not only is a TS analog but also exhibits various hydrogen bonds with the residues at the

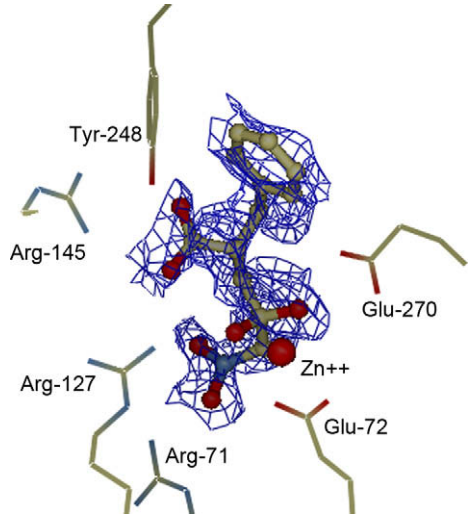

Figure 1. Difference electron density map for CPA-*R*-**5** complex generated with Fourier coefficient $|F_o| - |F_c|$ phases calculated from the final model omitting the bound inhibitor.

Table 2
Data collection and refinement statistics for the CPA-*R*-**5** complex

Space group	$P2_1$
Unit cell	
a, b, c (Å)	73.36, 59.75, 99.51
α, β, γ (°)	90.00, 104.04, 90.00
Resolution range (Å)	50.00–1.85
Number of unique reflections	67,762
Overall completeness (%)	89.6
R_{merge} (%)[a]	4.7
R factor[b]	23.6
Rms deviations[c]	
Bonds (Å)	0.005
Angles (°)	1.3
Dihedrals (°)	23.2

[a] R_{merge} for data sets for replicate reflections, $R = \sum||F_{hi}| - \langle|F_h|\rangle|/\sum\langle|F_h|\rangle|$, $|F_{hi}|$ = scaled structure factor for reflection *h* in data set *i*, $\langle|F_h|\rangle$ = average structure factor for reflection *h* calculated from replicate data.

[b] *R* factor, $R = \sum||F_o| - |F_c||/\sum|F_o|$; $|F_o|$ and $|F_c|$ are the observed and calculated structure factors, respectively.

[c] Rms: root mean square.

Table 3
Selected CPA-*R*-**5** interactions

Atom in *R*-**5**	Enzyme residue	Separation (Å)
O^1	Arg-145 guanidinium N^1	2.70
O^2	Tyr-248 phenolic O	2.62
O^3	Zn^{2+}	2.32
O^4	Zn^{2+}	2.42
O^3	Arg-127 guanidinium N^1	2.77
O^4	Glu-270 carboxylate O^1	2.59
O^5	Arg-127 guanidinium N^1	3.01
O^5	Arg-71 guanidinium N^1	2.81

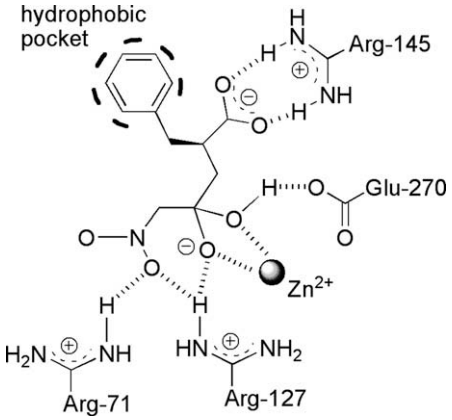

Figure 2. Schematic representation of the important interactions of *R*-**5** with the active site of CPA.

active site of CPA, which may be helpful to further development of new zinc proteases inhibitors.

Acknowledgement

The work was financially supported by the Science and Technology Committee of Jilin Province, China (No. 20060568).

References and notes

1. Babine, R. E.; Bender, S. L. *Chem. Rev.* **1997**, *97*, 1359.
2. Leung, D.; Abbenante, G.; Fairlie, D. P. *J. Med. Chem.* **2000**, *43*, 305.
3. Jacobsen, F. E.; Lewis, J. A.; Cohen, S. M. *ChemMedChem* **2007**, *2*, 152.
4. Lipscomb, W. N.; Sträter, N. *Chem. Rev.* **1996**, *96*, 2375.
5. Whittaker, M.; Floyd, C. D.; Brown, P.; Gearing, A. J. H. *Chem. Rev.* **1999**, *99*, 2735.
6. Ondetti, M. A.; Rubin, B.; Cushman, D. W. *Science* **1977**, *196*, 441.
7. Byers, L. D.; Wolfenden, R. *Biochemistry* **1973**, *12*, 2070.
8. Sugimoto, T.; Kaiser, E. T. *J. Am. Chem. Soc.* **1978**, *100*, 7750.
9. Christianson, D. W.; Lipscomb, W. N. *J. Am. Chem. Soc.* **1986**, *108*, 4998.
10. Jin, J.-Y.; Wang, S.-F.; Xuan, W.; Sheng, J.-W.; Wang, S.-H.; Tian, G. R. *Chin. J. Chem.* **2008**, *26*, 153.
11. Wang, S.-H.; Wang, S.-F.; Xuan, W.; Zeng, Z.-H.; Jin, J.-Y.; Ma, J.; Tian, G. R. *Bioorg. Med. Chem.* **2008**, *16*, 3596.
12. Compound *RS*-**5**: oil; IR (film): 3446, 1735, 1705, 1560 cm^{-1}; ^1H NMR (300 MHz, $CDCl_3$) δ 7.30–7.25 (m, 5H), 5.70 (s, 2H), 3.09 (dd, J = 5.4, 13.5 Hz, 1H), 2.93 (dd, J = 9.3, 17.4 Hz, 1H), 2.82 (dd, J = 8.3, 13.5 Hz, 1H), 2.65 (dd, J = 3.6, 17.4 Hz, 1H); ^{13}C NMR (75 MHz, $CDCl_3$) δ 195.5, 179.3, 137.4, 129.0, 128.9, 127.1, 83.2, 41.8, 39.9, 37.6. FT-ICR MS: Anal. Calcd for $C_{12}H_{13}NO_5$: 251.0794. Found: 250.0740 [M−H].Compound *R*-**5**: $[\alpha]_D^{20}$ = + 29.5 (*c*, 0.5, $CHCl_3$); FT-ICR MS: Anal. Calcd for $C_{12}H_{13}NO_5$: 251.0794. Found: 250.0743 [M−H].Compound *S*-**5**: $[\alpha]_D^{20}$ = −28.8 (*c*, 0.6, $CHCl_3$); FT-ICR MS: Anal. Calcd for $C_{12}H_{13}NO_5$: 251.0794. Found: 250.0744 [M−H].
13. Determination of K_i value. CPA was purchased from Sigma Chemical Co. (Allan form, twice crystallized from bovine pancreas, aqueous suspension in toluene) and used without further purification for kinetic assays. Lithium chloride and Tris were obtained from Sigma. *O*-(*trans*-*p*-Chlorocinnamoyl)-L-β-phenyllactate (Cl-CPL) was used as the substrate in the kinetic study. All solutions for kinetic study were prepared by dissolving in doubly distilled and deionized water. CPA stock solutions were prepared by dissolving CPA in 0.05 M Tris/0.5 M NaCl, pH 7.5 buffer solution and their concentrations were estimated from the absorbance at 278 nm (ε_{278} = 64,200). The stock assay solutions were filtered (GHP Acrodic syringe filter, pore size 0.2 μm) before use. Perkin–Elmer HP 8453 UV–vis spectrometer was used for UV absorbance measurements. The enzyme stock solution was added to a solution containing Cl-CPL (final concentrations: 50 and 100 μM) and inhibitor (five different final concentrations in the range of 0.5−2.0 K_i) in 0.05 M Tris/0.5 M NaCl, pH 7.5 buffer (1 mL cuvette), and the change in absorbance at 320 nm was measured immediately. The final concentration of CPA was 20 nM. Initial velocities were then calculated from the linear initial slopes of the change in absorbance where the amount of substrate consumed was less than 10%. The K_i values were then estimated from the semireciprocal plot of the initial velocity versus the concentration of the inhibitor according to the method of Dixon.[18]
14. Dean, J. A. In *Lange's Handbook of Chemistry*, 15th ed.; McGraw-Hill: New York, 1999.
15. CPA was washed three times with water to remove toluene used in packaging and then dissolved in 1.2 M LiCl. After centrifugation, the enzyme solution was then diluted to 12–15 mg/mL with a buffer solution of 1.2 M LiCl, 25 mM Tris, pH 7.5. An aliquot of this solution was then pipetted into a 100 μL glass dialysis button. A 7-kDa molecular weight cutoff membrane, which was pre-washed by doubly distilled and deionized water followed by equilibrated in 0.15 M LiCl, was placed over the button and secured with a rubber *O*-ring. The button was then dialyzed against 0.2 M LiCl, 25 mM Tris, pH 7.5, and at 4 °C. Crystals appeared after about 4 days on the bottom and edges of the well. The crystals were then crosslinked using a buffer solution containing 0.15 M LiCl and 0.02% (v/v) glutaraldehyde for 90 min. The crystals were then transferred to a soaking solution of the same buffer containing 50 μM racemic **5** and stored for 7 days in a cold room (4 °C) before data collection. Single crystals grew in the P_{21} space group with three molecules in one asymmetric unit. Crystallographic data were collected using a Rigaku RA-Micro 7 Desktop Rotating Anode X-ray Generator with a Cu target operating at 40 kV × 20 mA and R-Axis IV^{++} imaging-plate detector at a wavelength of 1.5418 Å. A 0.5-mm collimator was used to keep the whole crystal bathed in the X-ray beam. A total of 180 images with 1.0° oscillation were collected. The collected intensities were indexed, integrated, corrected for absorption, scaled and merged using *HKL* 2000. Diffraction images were processed with the CCP4 program suite. The structure of native CPA (PDB code 1M4L) was used as the starting model. The programs COOT[19] and CNS[20] were used in the model building and refinement, respectively. The randomly selected 5% of the data were set aside for the R_{free} calculation. Water molecules were gradually added to the model with CNS.
16. Christianson, D. W.; Lipscomb, W. M. *Acc. Chem. Res.* **1989**, *22*, 62.
17. Kim, H.; Lipscomb, W. N. *Biochemistry* **1990**, *29*, 5546.
18. Dixon, M. *Biochem. J.* **1953**, *55*, 170.
19. Emsley, P.; Cowtan, K. *Acta Crystallogr., Sect. D* **2004**, *60*, 2126.
20. Brunger, A. T.; Adams, P. D.; Clore, G. M. *Acta Crystallogr., Sect. D* **1998**, *54*, 905.